PAPER

Check for updates

Synthesis of biologically important tetrahydroisoquinoline (THIQ) motifs using quantum dot photocatalyst and evaluation of their anti-bacterial activity†

Jiteshkumar P. Deore and Mrinmoy De [ID] *

Our study introduces an efficient photocatalytic approach for synthesizing biologically significant C1-substituted tetrahydroisoquinoline (THIQ) motifs, employing WS_2 quantum dots (QDs) as catalysts. This method enables the formation of C−C and C−P bonds at the C1 position of the THIQ motif. The resulting compounds exhibit substantial antimicrobial activity against methicillin-resistant *Staphylococcus aureus* (MRSA) bacteria, with low minimum inhibitory concentration (MIC) values. Notably, the WS_2 QD catalyst demonstrates recyclability and suitability for gram-scale reactions, underscoring the sustainability and scalability of our approach. Overall, our research presents a versatile and cost-effective strategy for synthesizing C1-substituted THIQ derivatives, highlighting their potential as novel therapeutic agents in biology and medicinal chemistry.

Introduction

The tetrahydroisoquinoline (THIQ) based alkaloids, specifically 1-substituted THIQs have emerged as a crucial class of compounds with significant biological and pharmacological importance.[1] These alkaloids, found both in natural sources and through synthetic means, exhibit diverse biological activities and have been utilized in the development of drugs for the treatment of cancer, pain, gout, and neurodegenerative diseases.[2] (Fig. 1) The THIQ moiety, forming the backbone of these compounds, has attracted considerable attention in the scientific community, leading to the discovery of novel THIQ analogs with potent biological activity. Consequently, the development of synthetic methodologies for the synthesis of THIQ motifs holds immense biological significance and offers opportunities for the exploration of new therapeutic agents.[3]

Cross-coupling reactions are vital tools for the construction of biologically important organic molecules.[4] In the past, several methods, such as the Friedel–Crafts reaction, Michael addition, Aldol reaction, and nucleophilic substitution reactions, have been employed for C–C bond formation. However, the emergence of pericyclic reactions and transition metal-catalyzed reactions have revolutionized the field, boosted the efficiency of C–C bond formation, and substantially broadened

their scope.[5] Nevertheless, the high cost and toxic nature of some metals and the requirement of a specific activating group limit their applicability. In the last decade, photocatalysis has emerged as a promising alternative for transition metal-catalyzed reactions due to its energy-saving and environmentally friendly approach making it an attractive area of research in modern organic synthesis.[6]

Semiconductor quantum dots (QDs) have revolutionized photocatalysis by offering unique optoelectronic properties. Their exceptional photostability, high extinction coefficient, broad absorption spectra, and long-lived excited states make
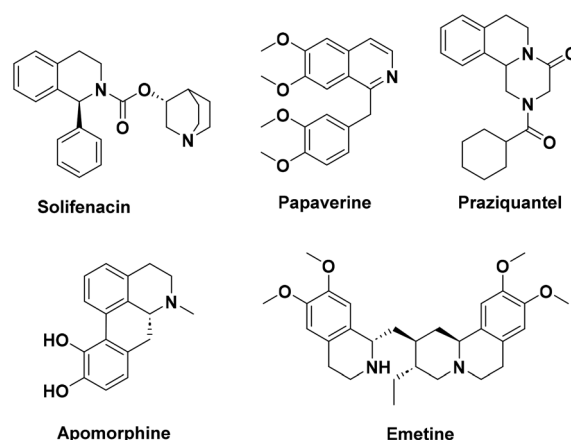
Department of Organic Chemistry, Indian Institute of Science, Bangalore-560012, India. E-mail: md@iisc.ac.in

†Electronic supplementary information (ESI) available. See DOI: **https://doi.org/10.1039/d3ob01305g**

Fig. 1 Biologically important THIQ motif.

This journal is © The Royal Society of Chemistry 2023

Org. Biomol. Chem., 2023, **21**, 9049–9053 | **9049**

them attractive alternatives to traditional organic dyes and metal-based photocatalysts.[7] Moreover, the size-dependent reduction and oxidation potentials of QDs can be adjusted, allowing tailored utilization for specific photochemical reactions.[8] QDs efficiently interact with organic molecules through charge transfer and/or energy transfer, rendering them highly effective for photocatalytic applications.[9] Among the extensively studied QDs, CdS, CdSe, WS$_2$, and MoS$_2$ stand out for their high quantum yield, stability and improved photocatalytic efficiency through enhanced light absorption, charge separation, and surface area.[10]

The functionalization of the C1 position of THIQ is a crucial step with significant implications in biology and medicinal chemistry.[11] Although numerous synthetic methods have been developed to accomplish this task, many of them rely on expensive catalysts and necessitate pre-functionalized starting materials or specific activating groups. Consequently, there is a pressing need for more cost-effective and versatile approaches. In this study, we demonstrate the efficient photocatalytic approach for synthesizing biologically important C1-substituted THIQ motifs, involving the formation of C–C and C–P bonds, leveraging the unique properties of semiconductor QDs. Furthermore, we assess the synthesized compounds through bioassays to evaluate their anti-bacterial activity, shedding light on their potential as novel therapeutic agents.
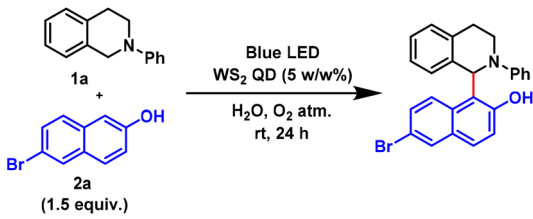
Results and discussion

CdSe, CdS, MoS$_2$, and WS$_2$ QDs were synthesized following established protocols to obtain their optimum size for enhanced catalytic performance. The synthesized QDs were characterized using transmission electron microscopy (TEM), UV-vis absorption, and fluorescence spectra analysis, confirming their expected coherence and properties (ESI†).

We initiated the optimization of reaction conditions for the functionalization of the C1 position of THIQ using a model substrate, *N*-phenyl THIQ, and 6-bromo-2-naphthol (Table 1). In our investigation, we screened various synthesized QDs including CdSe, CdS, MoS$_2$, and WS$_2$ to identify the most suitable catalyst for our reaction. Notably, we observed that WS$_2$ QDs exhibited a higher yield compared to the other tested QDs. Furthermore, we did a solvent screening experiment and determined that H$_2$O was the most compatible solvent with WS$_2$ QDs, leading to improved yield. Intriguingly, we observed no reaction yield in the absence of QDs, light source, or an O$_2$ atmosphere. This suggests that the reaction is mediated by visible light and that the QDs act as photocatalysts, while O$_2$ plays a vital role in regenerating the catalyst. We also determined that a 5 w/w% concentration of WS$_2$ QDs is sufficient to catalyze the reaction with a high yield.

After establishing an optimized condition, we proceeded to functionalize the THIQ motif using various naphthols, including 7-bromo and 6-methoxy derivatives. These reactions resulted in good yields of the desired products. Additionally, we explored the use of indoles with different substitutions to
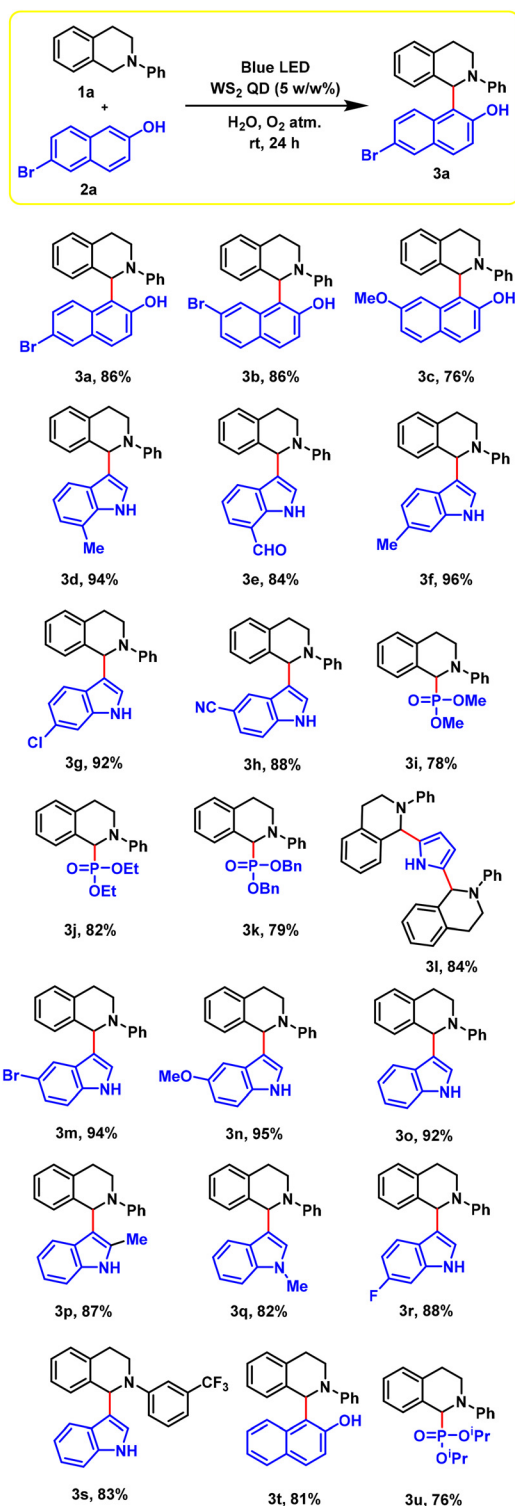
Table 1 Optimization of reaction condition

Sr. No.	Deviation from standard condition	Yield
1	None	82
2	3 w/w% QD	76
3	7.5 w/w% QD	83
4	1 equiv. of naphthol	74
5	2 equiv. of naphthol	83
6	H$_2$O : MeCN (1 : 1)	74
7	MeCN solvent	61
8	CdSe QD in chloroform	46
9	CdS QD in chloroform	52
10	Colloidal MoS$_2$ QD in MeCN	67

Reactions were carried out on 0.3 mmol scale of N-Ph THIQ and NMR yield are reported against terephthaldehyde internal standard.

forge a C–C bond at the C1 position of the THIQ motif, and observed high yields of the desired C1-functionalized products. The results indicate that double substitution occurred on the pyrrole moiety under the optimized conditions, likely due to the higher reactivity of the pyrrole at both the 2nd and 5th positions. Furthermore, we extended our optimized conditions to explore the formation of carbon-heteroatom (C–P) bonds at the C1 position of THIQ. Various phosphites were subjected to these reactions, resulting in the desired C1-functionalized products with satisfactory yields. This successful formation of C–P bonds further expands the synthetic versatility of the THIQ motif and offers additional opportunities for functionalization. These results collectively demonstrate the versatility and efficiency of our optimized conditions for the functionalization of the THIQ motif. The successful synthesis of C1-substituted THIQ derivatives using diverse substrates highlights the potential of our methodology for accessing structurally diverse compounds with potential biological activities (Scheme 1).

Several control experiments were conducted to gain insights into the reaction mechanism of our established methodology (Table 2). Initially, the reaction was performed in the presence of the radical scavenger 2,2,6,6-tetramethylpiperidine-1-oxyl (TEMPO) under standard optimized conditions (a). The results revealed that TEMPO slightly suppressed the reaction, leading to a yield of 56%. This observation suggests that the reaction proceeds through a Single Electron Transfer (SET) mechanism. On the other hand, the addition of electron scavenger Na$_2$CrO$_4$ and hole scavenger *N,N*-diisopropylethylamine (DIPEA) to the reaction did not significantly affect the yield (b & c). When the hole quencher *N,N*-diisopropylethylamine (DIPEA) was introduced into the standard optimized condition (c), a slight decrease in reaction yield was observed. Increasing the equi-

9050 | *Org. Biomol. Chem.*, 2023, **21**, 9049–9053

This journal is © The Royal Society of Chemistry 2023

Scheme 1 Substrate scope. Reactions were carried out on 0.5 mmol scale of N-Ph THIQ at optimized condition and isolated yield are reported after column chromatography.

valent of DIPEA correspondingly decreased the reaction yield, suggesting that WS$_2$ QD generates electron–hole pairs upon photo irradiation, and the hole quencher DIPEA acts as a catalyst poison for WS$_2$ QD.

Table 2 Mechanistic study

Expt. No.	Reaction Condition	Product yield (%)
a	In presence of 1 equiv. of TEMPO	56
b	In presence of 1 equiv. of Na$_2$CrO$_4$	79
c	In presence of 1 equiv. of DIPEA	74
d	Initial 1 h under light irradiation followed by 23 h under dark condition	<10
e	In absence of Blue LED	NR
f	In absence of MoS$_2$ QD	NR
g	In absence of Blue LED & WS$_2$ QD	NR
h	In absence of O$_2$ source	NR
i	In presence of 1 equiv. of DABCO	79

Equiv. Of DIPEA	0	1	2	3	4	6	8	9	10
Yield (%)	82	74	62	49	35	18	12	10	8

Condition: yield were determined by crude NMR against terephthaldehyde as internal standard.

Furthermore, the reactions were performed under different limiting conditions (e, f, g and h). Interestingly, the reactions ceased when any of the parameters were absent, indicating that WS$_2$ QD acts as a photocatalyst in the wavelength region of blue LED, and molecular oxygen is crucial for regenerating the catalyst. To further elucidate whether the reaction involves photo-redox catalysis or photo-energy transfer process, we performed the reaction in the presence of singlet oxygen quencher 1,4-diazabicyclo[2.2.2]octane (DABCO) (i). Surprisingly, we did not observe any significant changes in the reaction yield. This finding suggests that the formation of singlet oxygen does not occur during the reaction, thus ruling out the possibility of a photo-energy transfer process. It was found that reaction proceeding only when blue light was ON while it became ceased once the light OFF. It implies that reaction is mediated by visible light radiation and possibility of Chain Propagation pathway is ruled out. (Table 2, d).

Based on control experiments and previous literature reports, we have proposed a plausible mechanism for the observed reaction (Scheme 2). Upon photoirradiation, the ground state WS$_2$ quantum dots (QDs) are excited to the excited state WS$_2$ QD*. This excited state WS$_2$ QD* undergoes single electron transfer (SET) with the *N*-phenyl THIQ substrate (**1a**), resulting in the formation of the *N*-phenyl THIQ radical cation (**1b**). Concurrently, molecular oxygen (O$_2$) assists in the regeneration of the QD^{n-} to its ground state QD, while being reduced to the superoxide O$_2^{\bullet-}$ radical anion. Furthermore, the superoxide O$_2^{\bullet-}$ radical anion abstracts a hydrogen atom from the *N*-phenyl THIQ radical cation, leading to the formation of the *N*-phenyl THIQ iminium ion intermediate (**1c**) along with the generation of hydrogen peroxide (H$_2$O$_2$), which was confirmed by the starch iodine test. Subsequently, the desired nucleophile, β-naphthol (**2a**), attacks the iminium ion, resulting in the formation of the desired C1 functionalized product (**3a**).

Following the completion of the reaction, the WS$_2$ quantum dot (QD) catalyst was successfully recycled by transferring it

This journal is © The Royal Society of Chemistry 2023

Org. Biomol. Chem., 2023, **21**, 9049–9053 | **9051**
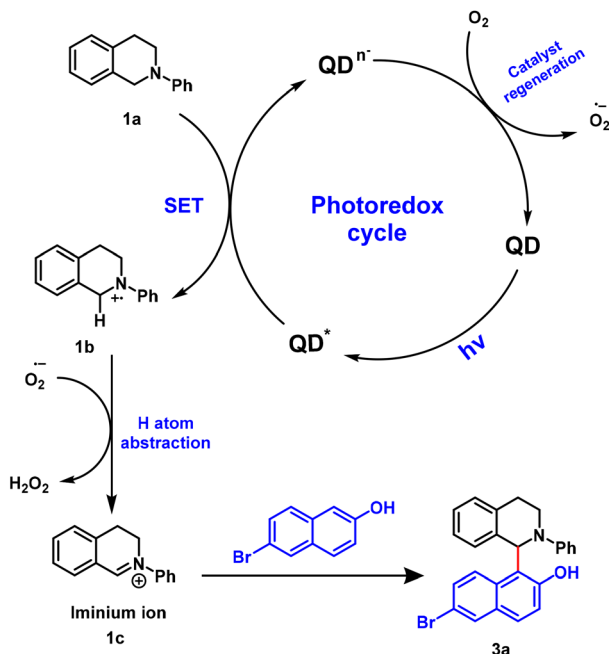
Scheme 2 Proposed mechanism.

Table 3 Bioactivity assay

Sr. No.	Compound	MRSA MIC (μg ml^{-1})
1	**3c**	60
2	**3d**	60
3	**3e**	No bioactivity
4	**3f**	60
5	**3g**	80
6	**3i**	80
7	**3j**	No bioactivity
8	**3k**	No bioactivity
9	**3l**	80

potential of specific C1-functionalized THIQ compounds, such as **3c**, **3d**, and **3f**, as promising candidates for further development as antibacterial agents against MRSA (Table 3).

Conclusions

In conclusion, our study demonstrates the efficient photocatalytic approach for synthesizing biologically important C1-substituted THIQ motifs. By leveraging the unique properties of semiconductor QDs, specifically WS$_2$ QDs, we achieved the formation of C–C and C–P bonds at the C1 position of the THIQ motif. The optimized conditions enabled the functionalization of THIQ with various naphthols, indoles and phosphites, resulting in the synthesis of desired C1-functionalized products with good yields. Furthermore, the synthesized compounds were evaluated for their antibacterial activity against Gram-positive MRSA, with compounds **3c**, **3d**, **3f** exhibiting significant antimicrobial effects at low MIC values. The recyclability of the WS$_2$ QD catalyst for multiple reaction cycles and its applicability in gram-scale reactions highlight the sustainability and scalability of our methodology. Overall, this study presents a versatile and cost-effective approach for the synthesis of C1-substituted THIQ derivatives and underscores their potential as novel therapeutic agents in biology and medicinal chemistry.

Author contributions

All authors contributed to the idea, design, execution of experiments and manuscript writing.

Conflicts of interest

There are no conflicts to declare.

Acknowledgements

from the organic ethyl acetate (EtOAc) layer into the aqueous layer. The recycled catalyst was then reused for subsequent reactions. The recyclability of the catalyst was assessed, and it demonstrated excellent sustainability for up to five cycles without any noticeable loss in reaction yield (Fig. 2.) and QD morphology (ESI S4†). Additionally, the methodology proved to be effective for gram-scale reactions, as illustrated in (Fig. 2).

At last, the antibacterial activity of the synthesized C1-functionalized THIQ motifs against Gram-positive bacteria methicillin-resistant *Staphylococcus aureus* (MRSA) was assessed using the broth dilution method. The minimum inhibitory concentration (MIC) values were determined by analyzing the growth curves (Fig. S2†). Among the nine compounds that are soluble in the aqueous solvent system, compounds **3c**, **3d** and **3f** exhibited notable antibacterial activity, with the lowest MIC value of 60 μg ml^{-1}. Additionally, compounds **3g**, **3i** and **3l** demonstrated antibacterial activity, albeit with a slightly higher MIC value of 80 μg ml^{-1}. However, compounds **3e**, **3j** and **3k** did not exhibit any significant antibacterial activity at concentrations up to 80 μg ml^{-1}. These findings highlight the
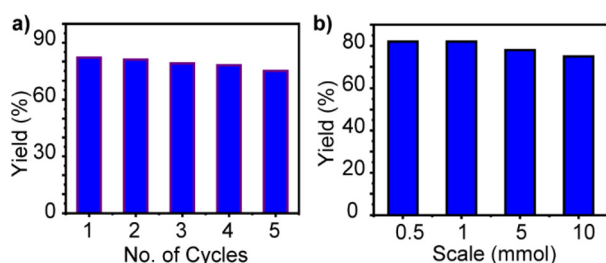

Fig. 2 (a) Recyclability test for catalyst (b) reaction scalability.

9052 | *Org. Biomol. Chem.*, 2023, **21**, 9049–9053

This journal is © The Royal Society of Chemistry 2023

References

1 J. D. Scott and R. M. Williams, *Chem. Rev.*, 2002, **102**, 1669–1730.

2 (*a*) R. K. Tiwari, D. Singh, J. Singh, A. K. Chhillar, R. Chandra and A. K. Verma, *Eur. J. Med. Chem.*, 2006, **41**, 40–49; (*b*) J. Zhu, J. Lu, Y. Zhou, Y. Li, J. Cheng and C. Zheng, *Bioorg. Med. Chem. Lett.*, 2006, **16**, 5285–5289; (*c*) A. Kumar, S. B. Katiyar, S. Gupta and P. M. S. Chauhan, *Eur. J. Med. Chem.*, 2006, **41**, 106–113; (*d*) X. H. Liu, J. Zhu, A. N. Zhou, B. A. Song, H. L. Zhu, L. S. Bai, P. S. Bhadury and C. X. Pan, *Bioorg. Med. Chem.*, 2009, **17**, 1207–1213; (*e*) J. J. Swidorski, Z. Liu, Z. Yin, T. Wang, D. J. Carini, S. Rahematpura, M. Zheng, K. Johnson, S. Zhang, P. F. Lin, D. D. Parker, W. Li, N. A. Meanwell, L. G. Hamann and A. Regueiro-Ren, *Bioorg. Med. Chem. Lett.*, 2016, **26**, 160–167; (*f*) A. M. Ehrenworth and P. Peralta-Yahya, *Nat. Chem. Biol.*, 2017, **13**, 249–258.

3 (*a*) W. M. Whaley and T. R. Govindachari, *Organic Reactions*, John Wiley & Sons, New York, 1951, vol. 6, p. 151; (*b*) R. P. Polniaszek and L. W. Dillard, *Tetrahedron Lett.*, 1990, **31**, 797; (*c*) D. L. Comins and M. M. Badawi, *Heterocycles*, 1991, **32**, 1869; (*d*) T. S. Kaufman, *J. Chem. Soc., Perkin Trans. 1*, 1996, **1**, 2497; (*e*) M. Schlosser, G. Simig and H. Geneste, *Tetrahedron*, 1998, **54**, 9023; (*f*) A. I. Meyers and D. A. Dickman, *J. Am. Chem. Soc.*, 1987, **109**, 1263; (*g*) G. Wei, C. Zhang, F. Bureš, X. Ye, C.-H. Tan and Z. Jiang, *ACS Catal.*, 2016, **6**, 3708–3712; (*h*) K. Jaiswal, G. Yarabahally, P. Behera and M. De, *ACS Org. Inorg. Au*, 2022, **2**, 205–213.

4 (*a*) J. Yamaguchi, A. D. Yamaguchi and K. Itami, *Angew. Chem., Int. Ed.*, 2012, **51**, 8960–9009; (*b*) C. Zheng and S.-L. You, *RSC Adv.*, 2014, **4**, 6173–6214.

5 (*a*) L. McMurray, F. O'Hara and M. J. Gaunt, *Chem. Soc. Rev.*, 2011, **40**, 1885–1898; (*b*) C. Liu, H. Zhang, W. Shi and A. Lei, *Chem. Rev.*, 2011, **111**, 1780–1824.

6 (*a*) D. Ravelli, S. Protti and M. Fagnoni, *Chem. Rev.*, 2016, **116**, 9850–9913; (*b*) C. S. Wang, P. H. Dixneuf and J. F. Soule, *Chem. Rev.*, 2018, **118**, 7532–7585; (*c*) M. H. Shaw, J. Twilton and D. W. MacMillan, *J. Org.*

Chem., 2016, **81**, 6898–6926; (*d*) L. Zhang, H. Yi, J. Wang and A. Lei, *J. Org. Chem.*, 2017, **82**, 10704–10709; (*e*) L. Marzo, S. K. Pagire, O. Reiser and B. König, *Angew. Chem., Int. Ed.*, 2018, **57**, 10034–10072; (*f*) Q. Q. Zhou, Y. Q. Zou, L. Q. Lu and W. J. Xiao, *Angew. Chem., Int. Ed.*, 2019, **58**, 1586–1604.

7 (*a*) M. Bruchez, M. Moronne, P. Gin, S. Weiss and A. P. Alivisatos, *Science*, 1998, **281**, 2013–2016; (*b*) W. C. W. Chan and S. Nie, *Science*, 1998, **281**, 2016–2018.

8 J. Jasieniak, M. Califano and S. E. Watkins, *ACS Nano*, 2011, **5**, 5888–5902.

9 (*a*) M. Malicki, K. E. Knowles and E. A. Weiss, *Chem. Commun.*, 2013, **49**, 4400–4402; (*b*) J. H. Olshansky, T. X. Ding, Y. V. Lee, S. R. Leone and A. P. Alivisatos, *J. Am. Chem. Soc.*, 2015, **137**, 2021–2029; (*c*) D. J. Weinberg, S. M. Dyar, Z. Khademi, S. R. Marder, M. R. Wasielewski and E. A. Weiss, *J. Am. Chem. Soc.*, 2014, **136**, 14513–14518.

10 (*a*) P. Linkov, V. Krivenkov, I. Nabiev and P. Samokhvalov, *Mater. Today: Proc.*, 2016, **3**, 104–108; (*b*) F. Wang, W. G. Wang, X. J. Wang, H. Y. Wang, C. H. Tung and L. Z. Wu, *Angew. Chem., Int. Ed.*, 2011, **50**, 3193–3197; (*c*) X. Xiang, L. Wang, J. Zhang, B. Cheng, J. Yu and W. Macyk, *Adv. Photonics Res.*, 2022, **3**, 2200065; (*d*) S. Xu, D. Li and P. Wu, *Adv. Funct. Mater.*, 2015, **25**, 1127–1136; (*e*) A. Manikandan, Y.-J. Chen, C.-C. Shen, C.-W. Sher, H.-C. Kuo and Y.-L. Chueh, *Prog. Quantum Electron.*, 2019, **68**, 100226; (*f*) M. M. Kandy, A. K. Rajeev and M. Sankaralingam, *Sustainable Energy Fuels*, 2021, **5**, 12–33.

11 (*a*) D. Taniyama, M. Hasegawa and K. Tomioka, *Tetrahedron: Asymmetry*, 1999, **10**, 221; (*b*) N. M. Gray, B. K. Cheng, S. J. Mick, C. M. Lair and P. C. Contreras, *J. Med. Chem.*, 1989, **32**, 1242; (*c*) K. Th. Wanner, H. Beer, G. Hofner and M. Ludwig, *Eur. J. Org. Chem.*, 1998, 2019–2029; (*d*) M. D. Rozwadowska, *Heterocycles*, 1994, **39**, 903; (*e*) R. P. Polniaszek, C. R. Kaufman and J. S. Meyers, *J. Am. Chem. Soc.*, 1989, **111**, 4859; (*f*) A. I. Meyers, J. S. Warmus, M. A. González, J. Guiles and A. Akahane, *Tetrahedron Lett.*, 1991, **32**, 5509; (*g*) B. Wünsch and S. Nerdinger, *Eur. J. Org. Chem.*, 1998, 711–718.

This journal is © The Royal Society of Chemistry 2023

Org. Biomol. Chem., 2023, **21**, 9049–9053 | **9053**